Journal of Power Sources 237 (2013) 167–171

Contents lists available at SciVerse ScienceDirect

Journal of Power Sources

journal homepage: www.elsevier.com/locate/jpowsour

Short communication

An in-situ copolymerization synthesis of $Li_3V_2(PO_4)_3$/C nanocomposite with ultrahigh discharge capacity

Wen-feng Mao [a,*], Ji Yan [a], Hui Xie [b], Zhi-yuan Tang [a], Qiang Xu [a]

[a] Department of Applied Chemistry, School of Chemical and Engineering, Tianjin University, Tianjin 300072, PR China
[b] Texas Materials Institute, ETC 9.184, University of Texas at Austin, United States

HIGHLIGHTS

- $Li_3V_2(PO_4)_3$/C has been firstly synthesized by an in-situ copolymerization method.
- The polyacrylamide as carbon source is firstly introduced into $Li_3V_2(PO_4)_3$/C system.
- The chelating reagent and copolymerization method is firstly combined.
- The $Li_3V_2(PO_4)_3$/C exhibits excellent cyclic performance at high discharge rates.

ARTICLE INFO

Article history:
Received 30 July 2012
Received in revised form
4 March 2013
Accepted 11 March 2013
Available online 19 March 2013

Keywords:
Lithium vanadium phosphate
In-situ polymerization
Core–shell structure
Lithium ion battery

ABSTRACT

High rate cathode $Li_3V_2(PO_4)_3$/C with an excellent electrochemical performance has been successfully synthesized via an in-situ copolymerization method. The synthesized $Li_3V_2(PO_4)_3$/C composite exhibits an extraordinary reversible discharge capacity of 103.1 mAh g^{-1} at 50 C discharge rate. In addition, there are no obvious capability fade after 100 cycles. The carbon from pyrolysis of polyacrylamide obtained from the in-situ copolymerization reaction is believed acting a critical role in acquiring such high performances.

1. Introduction

Recently, monoclinic NASICON-type lithium vanadium phosphate ($Li_3V_2(PO_4)_3$) as a promising candidate cathode material has attracted great interest owing to its stable structure, acceptable average voltage, low cost, safety and high theoretical capacity (197 mAh g^{-1}). Its special three-dimensional structure provides better ionic conductivity and outstanding rate capability than other phosphate materials. Therefore, the $Li_3V_2(PO_4)_3$ composite is expected to be the optimal cathode candidate for the high safety requirement of LIBs. However, the extraction of the third lithium ion at 4.55 V in $Li_3V_2(PO_4)_3$ is kinetically difficult and does adverse to its high rate capability [1–7]. Therefore the practical application of $Li_3V_2(PO_4)_3$ is usually cycled in the potential range of 3.0–4.3 V, delivering a theoretical capacity of 133 mAh g^{-1}.

On the other hand, inherent low electronic conductivity of $Li_3V_2(PO_4)_3$ severely hampers its practical application. Several strategies such as coating conductive material [8–12], doping ions [13–18] and preparing nano-scale particles [19–22] have been adopted to solve the problem. Among these methods, carbon coating has been confirmed as a simple and effective method. The coating-carbon can restrict the growth of $Li_3V_2(PO_4)_3$ primary particle effectively and results in well electronic conductivity.

Sol–gel method is promising route to synthesize carbon-coated $Li_3V_2(PO_4)_3$, since it offers possibility to coat carbon precursor homogeneously and control particle size in nano-scale [23–26]. For $Li_3V_2(PO_4)_3$, various kinds of sol–gel method are proposed using oxalic acid or citric acid as chelating agent [4,27]. But up to now, the cycling performance of $Li_3V_2(PO_4)_3$/C composite under high rate condition has remained unsatisfactory for potential industrial applications. There is still an urgent need for appropriate carbon coating processes to acquire structure-optimized $Li_3V_2(PO_4)_3$/C composite material with high discharge capacity, adequate cycling stability and acceptable cost.

* Corresponding author. Tel.: +86 83017180; fax: +86 769 83195372.
E-mail address: wenfengmao123@gmail.com (W.-f. Mao).

0378-7753/$ – see front matter © 2013 Elsevier B.V. All rights reserved.
http://dx.doi.org/10.1016/j.jpowsour.2013.03.039

Polyacrylamide is low-cost, and can disperse raw materials easily, especially it has amidocyanogens and acyls in the molecule, which can form complexes with metal ions among/in parallel polymer molecules, and then form a three-dimensional network among reactants. After carbonization, the three-dimensional network provides a better conductive network in favorable for the kinetic extraction/insertion reaction of Li^+ ions. However, to the best of our knowledge, there are no reports on using acrylamide as polymer monomer, N,N′-methylene-bisacrylamide as crosslinking agent and ammonium persulfate as initiator to prepare $Li_3V_2(PO_4)_3$/C composite.

In this paper, we firstly introduced a sol–gel method based on an in-situ copolymerization reaction to synthesize pure-phase and well-crystallized $Li_3V_2(PO_4)_3$/C with average particle size about 50 nm. The synthesized $Li_3V_2(PO_4)_3$/C composite exhibits high reversible capacity and good cycling performance over 100 cycles at different charge and discharge current densities.

2. Experimental

Stoichiometric amount of Li_2CO_3, V_2O_5 and $NH_4H_2PO_4$ were dispersed in 2–5 ml distilled water under continuous stirring for 30 min. Simultaneously, 2.83 g of citric acid, 0.71 g of acrylamide (AAM) and 0.15 g of N,N′-methylene-bisacrylamide (Bis) were dissolved into 8 ml distilled water and a transparent solution was formed. The solution was then added into the mixture of Li_2CO_3, V_2O_5 and $NH_4H_2PO_4$, and followed 0.1 mol L^{-1} ammonium persulfate (AP) was dropped into the mixture. The resultant batch was vigorously stirred for about 12 h under magnetic stirring. During this process, a free radical chain reaction is occurred between polymer monomer of AAM and crosslinking agent of Bis. After that, the resulting solution was heated at 80 °C until homogenous sol was formed. Finally, the sol was dried at 80 °C in vacuum oven, precalcined at 350 °C for 4 h and calcined at 800 °C for 8 h in N_2 atmosphere. The amount of residual carbon in the $Li_3V_2(PO_4)_3$/C composite was about 4.5%, based on the referred literature [9].

The structure of the as-prepared composite was characterized by X-ray diffraction (XRD, Rigaku D/max 2500v/pc) using Cu-Kα radiation from 10° to 60° at a scanning rate of 0.06° s^{-1}. The particle morphology and microstructure of the composite were observed with scanning electron microscopy (SEM, XL30ESEM, Philips) and transmission electron microscopy (TEM, JEM-2100F).

The electrochemical performances of the as-prepared composites were conducted by a composite electrode and measured using a coin cell. The cathode electrode was fabricated by mixing the obtained active powder, super P and polyvinylidene (PVDF) in a weight ratio of 85:10:5 in N-methyl-2-pyrrolidinone (NMP). The active material loading was about 3.6 mg cm^{-2} and the diameter of the electrode was 10 mm. The coin cells were assembled in an argon-filled glove box using lithium foil as anode electrode and 1 M $LiPF_6$ in EC/DMC (1:1, by volume ratio) as electrolyte. The galvanostatically charge and discharge tests were performed between 3.0 and 4.3 V at room temperature on a battery test system (NEWARE, BTS-610) under different current densities. Electrochemical impedance spectroscopy (EIS) measurements were carried out with a GAMRY PC14-750 electrochemical workstation in the frequency range of 10 kHz–10 mHz with an AC voltage of 5 mV.

3. Results and discussion

The in-situ copolymerization reaction plays an important role in obtaining high electrochemical performance $Li_3V_2(PO_4)_3$/C. During the copolymerization process (as shown in Fig. 1) [28], [$SO_4^{\bullet -}$] free radicals are firstly released from AP as the initiator of the chain reaction. With the existence of [$SO_4^{\bullet -}$], the copolymerization reaction is then activated between each AAM monomer. Simultaneously, the Bis acts as the crosslinking agent to form three-dimensional (3D) tangled network with the sheet or dendritic shape, as reported in the previous literature [29,30].

The X-ray diffraction pattern of the resulting $Li_3V_2(PO_4)_3$/C composite is shown in Fig. 2(a). The diffraction pattern matches well with the monoclinic $Li_3V_2(PO_4)_3$ phase (JCPDS Card No. 01-072-7074) with the space group of $P2_1/n$, although there are small amount of Li_3PO_4 (PDF#:15-0760) detected at about $2\theta = 18.0°$ and 22.4° [31,32]. In addition, no peak for crystalline carbon is observed, suggesting that the carbon in the composite is amorphous. The SEM image of the as-prepared composite is presented in Fig. 2(b). It shows that the $Li_3V_2(PO_4)_3$/C sample has an agglomeration morphology with the small primary particles. In order to investigate the inner microstructure of the $Li_3V_2(PO_4)_3$/C composite, the powder was analyzed by TEM measurement. From Fig. 2(c) and (d), it can be seen that the particle size of $Li_3V_2(PO_4)_3$ core ranges from 30 to 100 nm with the thickness of carbon shell about 1 nm. A relatively thin carbon layer is proven associated with carbonization of polyacrylamide and citric acid. It is believed that the carbon layer can effectively impede the secondary growth of primary $Li_3V_2(PO_4)_3$ as well as provide good electrical contact between the particles, beneficial for the high rate electrochemical performance.

Fig. 3(a) shows the 50th charge/discharge curves of the $Li_3V_2(PO_4)_3$/C composite at different discharge rates (5 C, 10 C, 20 C, 25 C, 30 C and 50 C) and 5 C charge rate. For the 5 C charge and discharge curves (1 C = 133 mAh g^{-1}), three plateaus at 3.62 V, 3.70 V and 4.12 V are observed, corresponding to a series of phase transition processes from $Li_3V_2(PO_4)_3$ to $Li_{2.5}V_2(PO_4)_3$, $Li_2V_2(PO_4)_3$

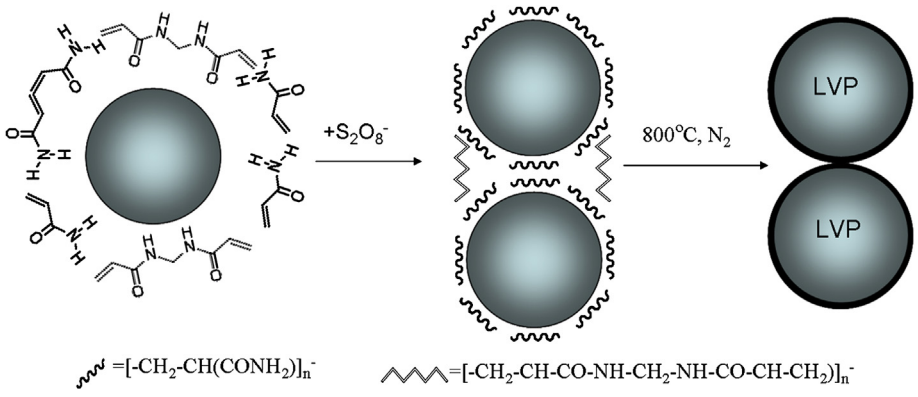

Fig. 1. Schematic diagram of the synthesis of core–shell structure cathode $Li_3V_2(PO_4)_3$/C composite.

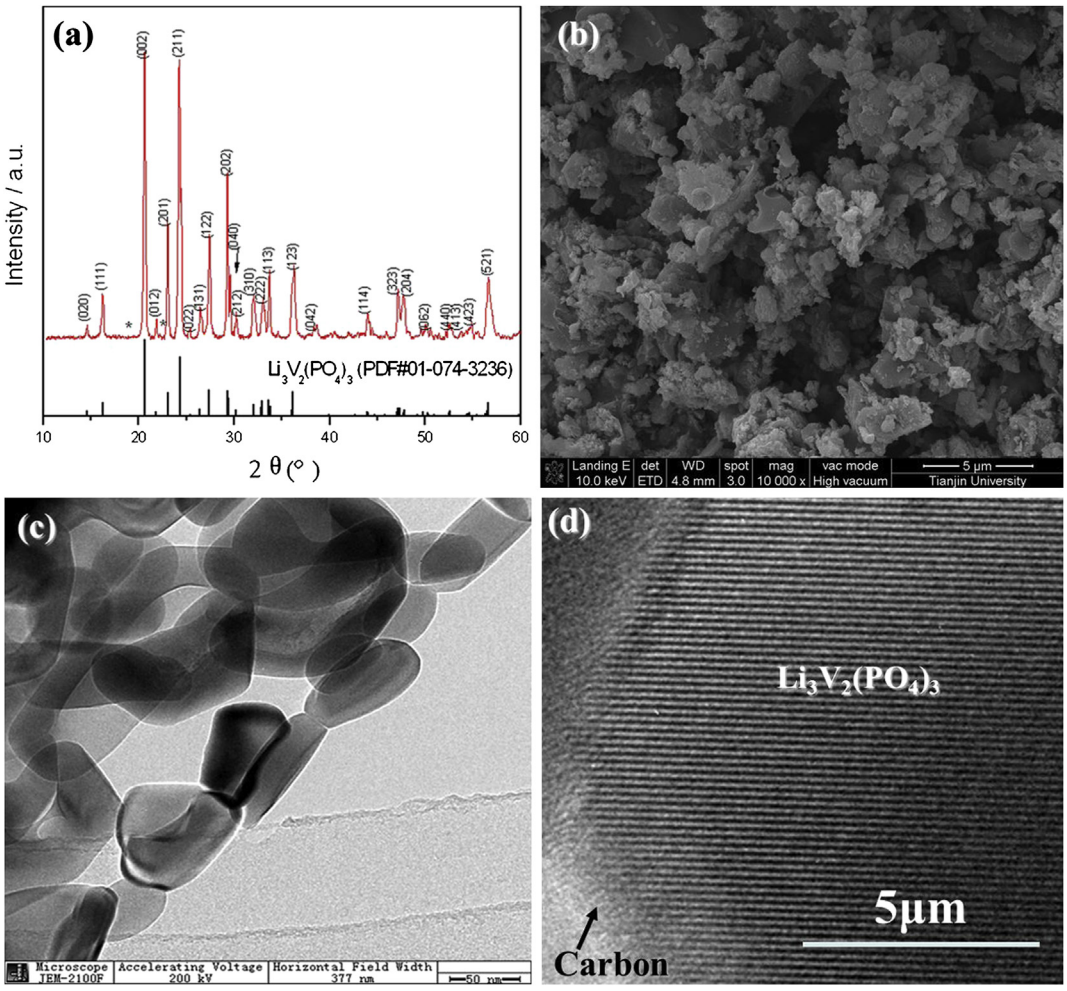

Fig. 2. XRD pattern (a), the SEM (b) and the TEM (c, d) of the as-prepared $Li_3V_2(PO_4)_3$/C composite.

and $LiV_2(PO_4)_3$, respectively [33]. During the charge process, the extraction of the first lithium ion at 3.6 V is divided into two steps because of the existence of an ordered phase $Li_{2.5}V_2(PO_4)_3$/C. Three corresponding discharge plateaus at 4.0 V, 3.63 V and 3.55 V are signed as the reinsertion of two lithium ions, accompanied with the sequence phase transition from $LiV_2(PO_4)_3$ to $Li_2V_2(PO_4)_3$, $Li_{2.5}V_2(PO_4)_3$ and $Li_3V_2(PO_4)_3$, respectively. A specific discharge capacity of 121.4 mAh g^{-1} is obtained at 5 C rate. Furthermore, the 3.6 g cm^{-2} of active material loading is higher than the 1.5 g cm^{-2} of the bulk $Li_3V_2(PO_4)_3$/C sample in the recent literature [33], although the specific discharge capacity is slightly lower. In comparison of the discharge curves of the $Li_3V_2(PO_4)_3$/C composite at different current densities, the potential differences between each couple are <0.2 V, indicating low polarizations and good ionic diffusion rates. When further operating at different discharge rates of 20 C and 30 C, the $Li_3V_2(PO_4)_3$/C composite presents specific capacities of 113.7 mAh g^{-1} and 105.2 mAh g^{-1}, respectively. More surprisingly, an unexceptionable discharge capacity of 103.1 mAh g^{-1} at a higher discharge rate of 50 C is still obtained. This is the highest discharge capacity under the similar active material loading and charge rate of 5 C. Fig. 3(b) shows the cycling performance of the $Li_3V_2(PO_4)_3$/C composite at different current densities. The discharge capacities stay very stable in the following cycles after the initial active cycle at 0.5 C charge/discharge rate. There is only small capacity decay of 2.32 mAh g^{-1}, 3.01 mAh g^{-1}, 5.5 mAh g^{-1}, 1.49 mAh g^{-1} after 100 cycles with the discharge rate increasing from 5 C to 10 C, 20 C, 25 C and 30 C, respectively; Even at 50 C discharge rate, a specific discharge capacity of 99.6 mAh g^{-1} is still obtained after 100 cycles with almost 100% of capacity retention, indicating the excellent cycling stability at such higher discharge rate.

Fig. 3(c) shows the excellent capacity recovering ability of the as-prepared $Li_3V_2(PO_4)_3$/C; only 8.0% capacity decay is observed after 200 cycles at different rates. The inset pattern of Fig. 3(c) reveals the charge/discharge curves after different numbers of cycles. The discharge capacity after a high rate of 30 C can retain almost the same value as that of the initial cycling at 5 C.

To further understand the ultrahigh rate performance of the composite, electrochemical impedance spectroscopy is studied. From Fig. 3(d), all spectra consist of a small depressed semicircle in high frequency range, a semicircle in middle frequency range and an inclined line in low frequency range. It is noted that the small depressed semicircle in high frequency range represents the resistance of SEI film [15] and the value almost maintains the same, indicating the stability of SEI film during cycling. With the increase of discharge rate from 5 C, 10 C, 20 C, 30 C and 5 C, the resistance in the middle frequency range gradually enlarges and then returns to relative low level. These results indicate that the electrochemical kinetic of $Li_3V_2(PO_4)_3$ is greatly improved with the utilizing the in-situ copolymerization route.

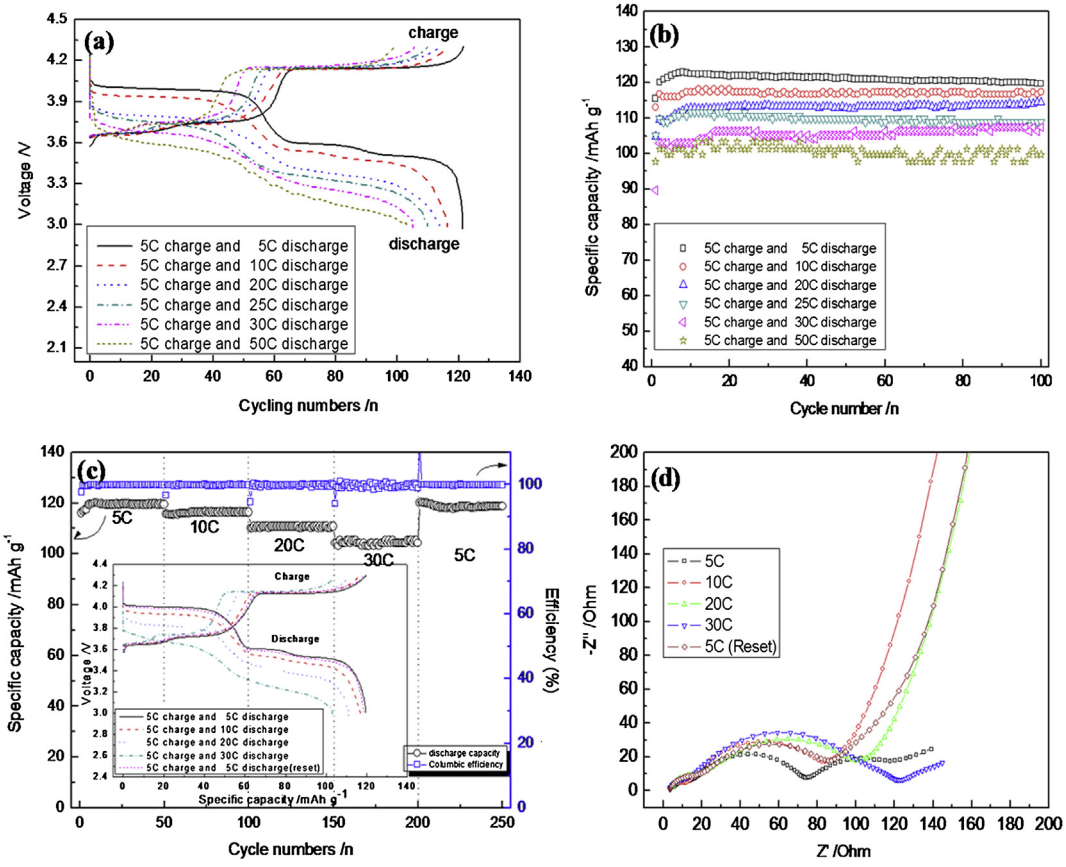

Fig. 3. Electrochemical performance of the synthesized $Li_3V_2(PO_4)_3$/C composites at different discharge rates. (a) and (b) are the typical charge/discharge curves and the corresponding cycling performances at the voltage range of 3.0–4.3 V; (c) the rate recovery of the $Li_3V_2(PO_4)_3$/C composite (inset the charge and discharge curves); (d) the Nyquist plots of the $Li_3V_2(PO_4)_3$/C composite after various cycling.

4. Conclusion

$Li_3V_2(PO_4)_3$/C composite cathode material with ultrahigh discharge capacity and excellent cycling performance was synthesized by an in-situ copolymerization method. Nano-sized particles with a core–shell structure and a thin-layer carbon coating were obtained. The as-prepared $Li_3V_2(PO_4)_3$/C presents an excellent high rate capability of 103.1 mAh g^{-1} at a discharge rate as high as 50 C with the active material loading of 3.6 g cm^{-1} and also a high capacity retention was achieved. The extraordinary high-rate performances of the $Li_3V_2(PO_4)_3$/C would be attributed to (i) the nanoscale of the primary particles, (ii) the chelating effect of citric acid and (iii) the encapsulation of 3D-structure of carbon precursor to the metal ion during the in-situ copolymerization process.

Acknowledgment

This work is supported by National Science Foundation of China (Grant No. 20973124)

References

[1] H. Huang, S.-C. Yin, T. Kerr, N. Taylor, L.F. Nazar, Advanced Materials 14 (2002) 1525–1528.
[2] A. Pan, J. Liu, J.-G. Zhang, W. Xu, G. Cao, Z. Nie, B.W. Arey, S. Liang, Electrochemistry Communications 12 (2010) 1674–1677.
[3] L. Wang, L.-C. Zhang, I. Lieberwirth, H.-W. Xu, C.-H. Chen, Electrochemistry Communications 12 (2010) 52–55.
[4] L. Wang, Z. Tang, L. Ma, X. Zhang, Electrochemistry Communications 13 (2011) 1233–1235.
[5] L. Su, Y. Jing, Z. Zhou, Nanoscale 3 (2011) 3967–3983.
[6] M. Hu, J. Wei, L. Xing, Z. Zhou, Journal of Power Sources 222 (2013) 373–378.
[7] K. Nagamine, T. Honma, T. Komatsu, Journal of Power Sources 196 (2011) 9618–9624.
[8] Y.Q. Qiao, X.L. Wang, J.Y. Xiang, D. Zhang, W.L. Liu, J.P. Tu, Electrochimica Acta 56 (2011) 2269–2275.
[9] X.H. Rui, C. Li, J. Liu, T. Cheng, C.H. Chen, Electrochimica Acta 55 (2010) 6761–6767.
[10] L. Zhang, X.L. Wang, J.Y. Xiang, Y. Zhou, S.J. Shi, J.P. Tu, Journal of Power Sources 195 (2010) 5057–5061.
[11] Y.Q. Qiao, J.P. Tu, X.L. Wang, C.D. Gu, Journal of Power Sources 199 (2012) 287–292.
[12] Y.Q. Qiao, J.P. Tu, X.L. Wang, D. Zhang, J.Y. Xiang, Y.J. Mai, C.D. Gu, Journal of Power Sources 196 (2011) 7715–7720.
[13] C. Deng, S. Zhang, S.Y. Yang, Y. Gao, B. Wu, L. Ma, B.L. Fu, Q. Wu, F.L. Liu, The Journal of Physical Chemistry C 115 (2011) 15048–15056.
[14] Y. Xia, W. Zhang, H. Huang, Y. Gan, C. Li, X. Tao, Materials Science and Engineering: B 176 (2011) 633–639.
[15] Q. Chen, X. Qiao, Y. Wang, T. Zhang, C. Peng, W. Yin, L. Liu, Journal of Power Sources 201 (2012) 267–273.
[16] S. Zhong, L. Liu, J. Liu, J. Wang, J. Yang, Solid State Communications 149 (2009) 1679–1683.
[17] M. Ren, Z. Zhou, Y. Li, X.P. Gao, J. Yan, Journal of Power Sources 162 (2006) 1357–1362.
[18] S. Zhang, Q. Wu, C. Deng, F.L. Liu, M. Zhang, F.L. Meng, H. Gao, Journal of Power Sources 218 (2012) 56–64.
[19] A. Pan, D. Choi, J.-G. Zhang, S. Liang, G. Cao, Z. Nie, B.W. Arey, J. Liu, Journal of Power Sources 196 (2011) 3646–3649.
[20] Y.Q. Qiao, X.L. Wang, Y.J. Mai, J.Y. Xiang, D. Zhang, C.D. Gu, J.P. Tu, Journal of Power Sources 196 (2011) 8706–8709.
[21] M.M. Ren, Z. Zhou, X.P. Gao, W.X. Peng, J.P. Wei, The Journal of Physical Chemistry C 112 (2008) 5689–5693.
[22] Q. Kuang, Y. Zhao, Journal of Power Sources 216 (2012) 33–35.
[23] Y.-Z. Li, Z. Zhou, M.-M. Ren, X.-P. Gao, J. Yan, Materials Letters 61 (2007) 4562–4564.
[24] Y. Li, Z. Zhou, X. Gao, J. Yan, Electrochimica Acta 52 (2007) 4922–4926.
[25] Y. Li, Z. Zhou, M. Ren, X. Gao, J. Yan, Electrochimica Acta 51 (2006) 6498–6502.

[26] H. Wang, Y. Li, C. Huang, Y. Zhong, S. Liu, Journal of Power Sources 208 (2012) 282–287.
[27] W. Yuan, J. Yan, Z. Tang, O. Sha, J. Wang, W. Mao, L. Ma, Journal of Power Sources 201 (2012) 301–306.
[28] M. Szwarc, M. Levy, R. Milkovich, Journal of American Chemistry Society 78 (1956) 2656–3257.
[29] H. Zhang, X. Fu, S. Niu, G. Sun, Q. Xin, Journal of Solid State Chemistry 177 (2004) 2649–2654.
[30] A. Tarancón, G. Dezanneau, J. Arbiol, F. Peiró, J.R. Morante, Journal of Power Sources 118 (2003) 256–264.
[31] W.-f. Mao, J. Yan, H. Xie, Z.-y. Tang, Q. Xu, Electrochimica Acta 88 (2013) 429–435.
[32] W.-f. Mao, J. Yan, H. Xie, Y. Wu, Z.-y. Tang, Q. Xu, Materials Research Bulletin 47 (2012) 4527–4530.
[33] L. Zhang, H. Xiang, Z. Li, H. Wang, Journal of Power Sources 203 (2012) 121–125.